

Biodiesel blends for eco-friendly CRDI-VCR engines: enhancing combustion and engine performance to minimize pollutant emissions

Anbarasan Baluchamy^{1*}, Sakthi Rajan C.², Balamurugan S.³ and Venkatesh J.⁴

¹Department of Mechanical Engineering, PSNA College of Engineering and Technology, Dindigul 624 622, Tamil Nadu, India

²Department of Mechanical Engineering, SBM College of Engineering & Technology, Dindigul 624 005, Tamil Nadu, India

³Department of Mechanical Engineering, Chennai Institute of Technology, Kundrathur, Chennai, 600 069 Tamil Nadu, India

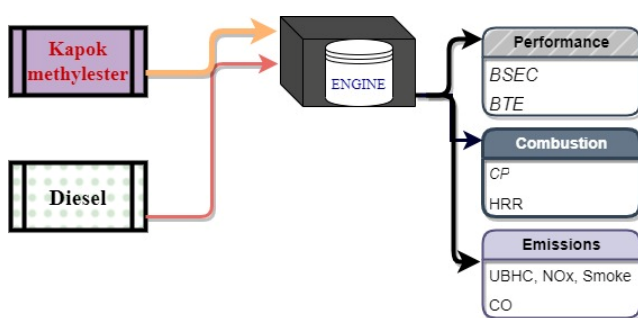
⁴Department of Mechanical Engineering, Dr. Mahalingam College of Engineering and Technology, Pollachi, 642 003, Tamil Nadu, India

Received: 28/01/2024, Accepted: 12/02/2024, Available online: 26/02/2024

*to whom all correspondence should be addressed: e-mail: anbarasan5mech@gmail.com

<https://doi.org/10.30955/gnj.005777>

Graphical abstract



Abstract

Energy is essential but associated with global greenhouse emissions. Therefore, clean and renewable energy is important for future development. To meet this demand, kapok oil methyl ester (KOME) was made from the kapok raw oil through the transesterification method. KOME was then combined with diesel in the ratios of 10%, 20%, and 30% (v/v%) to form KOME10, KOME20, and KOME30 mixtures. The combustion and emissions outcomes of KOME blends were studied at a stationary DI engine under different loads and modified common rail direct injection (CRDI) mode at 400 bar injection pressure, partial load, and CR of 19:1, 20:1, and 21:1. The combustion analysis of blends like maximum pressure (P_{max}) and net heat release rate (HRR_{max}) were observe lesser than diesel at stationary mode, whereas they increased by 13–15% and 16–32% in CRDI mode, respectively. Exhaust from engine such as carbon dioxide, hydrocarbons, and smoke were decreased, but nitric oxide increased about 0.7–1.5% and 1.3–8% for stationary and CRDI modes, respectively, as compared to diesel. This concludes that KOME might be a suitable substitute to diesel fuel for non-road DI engine applications.

Keywords: Kapok biodiesel, CRDI engine, VCR engine, combustion, emissions

Abbreviations

| | | | |
|--------------------|------------------------------|-----------------|------------------------------|
| bTDC | before top dead centre | IP | Injection pressure |
| CR | Compression ratio | KOME | Kapok oil methyl ester |
| CRDI | Common rail direct injection | KOME 10 | 10% KOME and 90% Diesel |
| CV | Calorific value | KOME 20 | 20% KOME and 80% Diesel |
| CN | Cetane number | KOME 30 | 30% KOME and 70% Diesel |
| CAD | Crank angle degree | MUFA | Mono-unsaturated fatty acids |
| CD | Combustion duration | NO _x | Nitrogen oxide |
| CO | Carbon monoxide | P_{max} | Maximum peak pressure |
| CO ₂ | Carbon dioxide | PCP | Premixed combustion phase |
| DCP | Diffusion combustion pahse | PUFA | Poly-unsaturated fatty acids |
| EoC | End of combustion | P_{cyl} | In-cylinder pressure |
| HC | Hydro carbon | SFA | Saturated fatty acids |
| HRR | Heat released rate | SOC | Start of combustion |
| HRR _{max} | Maximum heat released rate | TDC | Top dead centre |
| ID | Ignition delay | T_{cyl} | In-cylinder temperature |

1. Introduction

Transportation plays a vital part in any economy. Many developed countries, are focussing on vehicle electrification to convert all Internal combustion (IC) engine vehicles into electric vehicles (Sharma *et al.* 2022a).

The reduction of environmental pollution is the goal of promoting electric vehicles. Internal combustion (IC) engines are still a viable alternative, despite the potential benefits of electric cars (Azad *et al.* 2023). Due to their inadequate infrastructure, adopting electric car technology is extremely difficult in the majority of developing nations (Azad *et al.* 2023, Hoang *et al.* 2023). In majority of developing nations, coal is the primary energy source for

power production. In order to meet increasing consumer demand, more electricity must be produced, which will increase environmental pollution as most economies don't have access to renewable power resources (Yilbasi *et al.* 2023). Renewable fuels are crucial for sustainable development, boosting economic growth, and lowering environmental pollution (Al-Ansari *et al.* 2023).

Table 1. Engine performance compared to diesel fuel

| Engine type | Operating condition | Type of biodiesel fuel | Performance (BTE%) | Emissions | | | Ref. |
|---|--|------------------------|--------------------|-----------|-------|---------|-----------------------------------|
| | | | | NOx | HC | CO | |
| 1cyl., WC, DI, P 3.5 kW, CR 17.5:1 | Variable loads, @ 1500 rpm. Blends L5, L10, L15 & L20 | Linseed | ↑ 10–12% | ↑ 4% | ↑ 2% | ↑ 2% | (Jindal and Salvi 2012) |
| 1cyl., WC, 4S, DI, P 3.5 kW, CR 16.5:1 | Variable loads, @ 1500 rpm, Blends N5, N10, N15 & N20 | Neem | ↑ with B5 and B10 | ↑ 7% | ↑ | ↓ 2.5% | (Sivalakshmi and Balusamy 2012) |
| 2 cyl., WC, 4S, DI, P 26HP, CR 16.4:1, 1500 rpm | Different speed (1000-1900) at full load | Jojoba | ↑ @ 1900rpm | ↑ 16% | ↑ | ↑ 5% | (Saleh 2009) |
| 1cyl., AC, 4S, DI, P 6.25 kW, CR 178:1, 3600 rpm | Max load at different speed (1700, 2000, 2300, 2600 & 3000 rpm) | Cottonseed | ↑ 6% with B20 | ↑ ~7% | | ↓ 15% | (Hazar 2010) |
| 1cyl., WC, 4S, DI, P 5.5 kW, CR 16.5:1, 1500 rpm | Speed 1500 rpm @ different load | Rubber seed | 4.9 % ↓ lower | ↑ ~6% | ↓ 2% | ↓ 0.37% | (Sriram <i>et al.</i> 2023) |
| 1cyl., AC, DI, P 9 kW, CR 18:1 | M20, M40, M60 & M80 at different load, 1500 rpm | Mahua Indica | ↑ 1% with B20 | ↑ ~6% | | ↓ 0.2% | (Raheman and Ghadge 2007) |
| 1cyl., WC, 4S, DI, P 5.2 kW, CR 17.5:1, 1500 rpm injection pressure 220 bar | Blend, PK25, PK50, PK17 & PK100 at various load condition | Pine Kapok | ↑ 2% with B25 | ↑ ~9% | ↑ ~2% | ↓ 0.1% | (Vallinayagam <i>et al.</i> 2014) |
| 1cyl., WC, 4S, DI, P 3.5 kW, CR 17.5:1, 1500 rpm | Blends K10, K20, K50 & K75 @ different load | Karanja | ↑ 1% with B10 | ↑ ~5% | ↑ ~2% | ↑ 0.4% | (Sharma <i>et al.</i> 2021) |
| 1cyl., WC, 4S, DI, P 7.5 kW, CR 17.5:1, 1500 rpm DAF 10 model, | Blends J5, J10, J20, J30 @ different loads | Jatropha | ↑ with B10 | ↑ 2-5% | ↑ ~2% | ↓ 0.4% | (Chauhan <i>et al.</i> 2012) |

Biofuel is a plant-based substitute to fossil fuel, that has the possible to decrease carbon dioxide (CO₂), CO and PM emissions by CI engines (Jin and Wei 2023). Biodiesel, are mono-alkyl esters derived from oil feedstocks or animal fats, and are a sustainable alternative to fossil diesel fuel (Winangun *et al.* 2023). They are produced through the chemical process of transesterification. Biodiesel has many advantages over diesel fuel, such as integral lubricant, less toxic, biodegradability, negligible sulfur content and inferior CO₂ emissions (Luo *et al.* 2023; Ali and Maki 2023). Utilization of biodiesel is a way to diminish reliance on fossil fuel and the downside environmental impacts of fossil fuel combustion, while at the same time improving rural employment (Kumar and Paul 2023; Tutak *et al.* 2023). The Indian government encouraged the role that developing

biofuel, particularly from non-edible oil feedstocks on marginal or degraded soils, might play in establishing a thriving new rural sector (Sharma *et al.* 2022a; 2022b). Wang *et al.* (2013), investigated fuel preparation from Waste cooking oil (WCO). They proposed a new method to produce biodiesel through enzymatic esterification. WCO was utilized for the research. Hydrolysis process was used to reduce the fatty acids by using urea to hydrolyse WCO with water (Wang *et al.* 2014). This method reduced the unsaturation of WCO and improved the yield percentage of the biodiesel (Wang *et al.* 2014). A hydrolyzed WCO was transesterified with iso-propanol for biodiesel production. Fuel properties were investigated and an improvement in low-temperature fuel properties was reported (Wang *et al.* 2014).

Available studies in the literature (Hoang *et al.* 2023; Al-Ansari *et al.* 2023; Jin and Wei 2013; Winangun *et al.* 2023; Luo *et al.* 2023; Ali and Maki 2023; Kumar and Paul 2023; Tutak *et al.* 2023; Tongroon *et al.* 2023) has been found to exhibit higher levels of NO_x emissions, although other pollutants are generally lower compared to conventional diesel fuel. Mohammed El-Adawy *et al.* (2018), studied the outcome of increases in the air intake charge and CR (14:1, 16:1 and 18:1) on automotive engines fuelled with biodiesel. The study reported that at higher CR 18:1, engine performance increased with increased air intake charge by using a supercharger (El-Adawy *et al.* 2018). The supercharger reduces the BSFC by increasing the intake air charge density (El-Adawy *et al.* 2018). The compression increases the density and temperature of the intake air thus improving the combustion efficiency of viscous biodiesel. A similar study was performed by Mohammed EL Kassaby *et al.* (El_Kassaby and Nemit_allah 2018), that examined the influence of different methylester and diesel blends like as 10% (10% biodiesel+90% diesel), 20%, 30% and 50% by varying the CRs 14, 16 and 18. They reported that engine torque for all the blend samples was increased by increasing the CR (El_Kassaby and Nemit_allah 2018). They reported that at all the CRs; BSFC increased with increases biodiesel % in the blend due to a reduction in calorific value. Moreover, BTE for the 10%, 20%, 30% and 50% blend samples increased by 18.39%, 27.48%, 18.5 % and 19.82% at all CRs (El_Kassaby and Nemit_allah 2018). They also indicated that the emission of CO₂ and NO_x rise, while the emission of UBHC, CO and smoke opacity decreased at the CRs 14:1, 16:1 and 18:1 (El_Kassaby and Nemit_allah 2018). Channappagoudra *et al.* (2018), investigated the effect dairy scum oil biodiesel at different compression ratio (CR 16, CR17 and CR18) in a stationary engine. Authors observed that with increased CRs the engine performance was improve. Higher CR also enhanced combustion, such as maximum pressure, and total HRR and lowered the engine out pollutions of CO, HC, NO_x and smoke at higher CR (Channappagoudra and Ramesh 2018).

From Table 1, it can be inferred that many studies have been done on different feedstock biodiesel in an unmodified diesel engine. Based on the literature study, it was found that a comparative study of kapok oil biodiesel in stationary and modified common rail direct-inject (CRDI) mode has not been proposed anywhere yet. The present study is aim to see the compatibility of KOME in same size engines but different in operating mode. Therefore, to fulfil this research gap, an experimental investigation of kapok oil methyl ester (KOME) biodiesel has been conducted on stationary and modified CRDI modes to analysed combustion and emissions characteristics. The high cultivation of kapok seeds are mainly in Africa, Asia, Central America and Austrial. Thus, this research may improved the opportunity for the local farmers specially for Africa and Aisa to produced their own low carbon sustainable energy for agriculture and storage.

2. Materials and methods

2.1. Biodiesel production

The transesterification reaction process was used in a college lab to synthesize kapok oil methylester, as shown in Figure 1. Equations 1 and 2 (Sharma and Duraisamy 2019) were used to determine that the initial free fatty acid concentration in kapok seed oil was 2.3%. The value dropped below the permitted limit of 2.5%, which allowed the transesterification reaction to occur. The biodiesel synthesis process involved using a molar ratio of 6:1 of methanol to oil, along with a 1% (wt/wt%) application of the base catalyst Potassium hydroxide to pre-heated oil at a temperature of 65°C. A constant speed of 400 rpm was used to swirl the combined ingredients for 90 minutes (Sharma *et al.* 2019). Subsequently, the mixture was transferred to a separating flask and allowed to stand for a maximum duration of 10 hours to promote the separation of glycerol. The post-treatment procedure entailed the use of de-ionized hot water (70–80°C) to eradicate soap and any remaining methanol. Following a comprehensive cleaning process, the oil was subjected to heating at a temperature of 90°C while being purged with nitrogen for a duration of 15 minutes in order to eliminate any residual moisture. Raw glycerol was used to make soap cakes for washing and methanol was stored for later use.

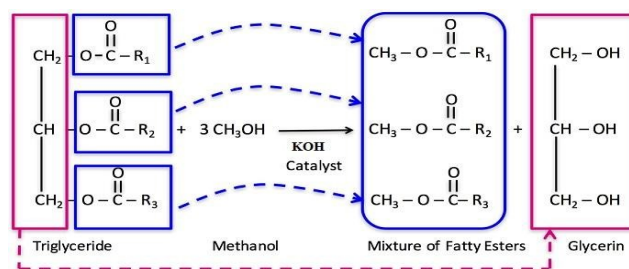


Figure 1. Transesterification of Triglycerides with Alcohol obtained from (Sharma and Duraisamy 2019)

2.2. Biodiesel fuel characterisation

Table 2 shows the physiochemical properties of KOME and blended fuels, all of which comply with the American standard (ASTM D7042) (Sharma *et al.* 2019). The ASTM D7042 method was utilized to ascertain the viscosity of KOME. This viscosity plays a significant role in the flow of gasoline, as it causes resistance in the fuel line when subjected to shear or tensile stress. Viscosity also affects the characteristics of fuel spray and combustion. The ASTM 4052 standard was used for KOME's density measurement, and a bomb calorimeter and the ASTM 4868 standard procedure were used to determine the calorific value. The calorific value (CV) acts as a measure of the fuel's energy input (Sharma *et al.* 2019). As a result of the presence of oxygen molecules, biodiesel has a CV that is typically lower than that of diesel fuel. Equations 3 and 4 were used to determine the cetane index (CI), a near approximation of the cetane number (CN) (Sharma *et al.* 2021). CN represents the fuel's ability to ignite spontaneously, with a higher CN suggesting a greater ease of autoignition. The flash point of KOME biodiesel was determined using a closed-cup flash point equipment that was operated manually. GC-MS was used to assess the content and proportion of fatty acids in KOME as shown in Figure 2. Equations 5, 6, and 7 calculated SFA, MUFA, and PUFA percentages (Sharma and Duraisamy 2019; Sharma *et al.*

2019). Please refer to the references that have been provided (Sharma and Duraisamy 2019; Sharma *et al.* 2019) for more in-depth steps in the calculating process.

$$\text{Cetane Index} = \frac{\text{Aniline Point}(^{\circ}\text{F}) \times \text{Degree of API}(60^{\circ}\text{F})}{100} \quad (3)$$

$$\text{Cetane Number} = 0.72 \times \text{CI} + 10 \quad (4)$$

$$\text{SFA \%} = \Sigma C - C \text{ single bond FAs} \quad (5)$$

$$\text{MUSFA \%} = \Sigma \text{More than one } (-C - C -) \text{uble bond FAs} \quad (6)$$

$$\text{PUSFA \%} = \Sigma \text{More than one } (-C = C -) \text{uble bond FAs} \quad (7)$$

Table 2. The physicochemical properties of KOMÉ biodiesel compared to standards

| Properties | Unit | Biodiesel ASTM D6751 | Diesel | KOME | KOME10 | KOME20 | KOME30 |
|------------------------|--------------------|----------------------|--------|-------|--------|--------|--------|
| Specific gravity(40°C) | | 0.88 | 0.830 | 0.875 | 0.845 | 0.866 | 0.882 |
| Density (40°C) | Kg/m ³ | 0.84- 0.90 | 830 | 875 | 845 | 866 | 882 |
| Viscosity (40°C) | mm ² /s | 1.50- 6.00 | 2.3 | 4.4 | 2.40 | 2.85 | 3.2 |
| Calorific Value | MJ/m ³ | - | 44.50 | 36.29 | 43.30 | 41.85 | 40.62 |
| Cetane Number | - | 48-60 | 52 | 54 | 54 | 56 | 58 |
| Acid Number | mgKOH/g | max 0.50 | - | 0.2 | 0.033 | 0.064 | 0.085 |
| FFA | % | max 0.50 | - | 0.1 | - | - | - |
| Fire point | (°C) | - | 50 | 170 | 70 | 89 | 98 |
| Flash Pont | (°C) | - | 45 | 156 | 65 | 76 | 88 |
| SFA% | | | - | 26 | - | - | - |
| MUFA% | | | 44 | - | - | - | - |
| PUFA% | | | 13 | - | - | - | - |

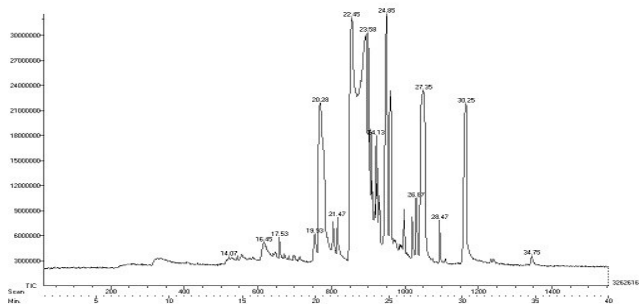


Figure 2. GC-MS spectrum of KOMÉ

2.3. Engine experimental setup

A stationary single-cylinder engine with a variable compression ratio (VCR) between 5:1 and 22:1 was selected for this investigation. Table 2 shows the engine's eddy current dynamometer, cylinder pressure transducer, cran angle encoder, air surge tank with manometer, and MAP sensor. The stationary engine was then modified to become a CRDI diesel engine, as seen in Figure 3. Table 2 provides a full description of the specifications and operating characteristics for both engine variants. The traditional mechanical fuel injection system was substituted with a CRDI fuel system, which integrates a common rail and electronic fuel injection capable of consistently maintaining a fuel injection pressure (IP) between 250 and 700 bar. The CRDI system was controlled using an accessible electronic control unit. The National Instruments NI-DAQ data collecting system was utilized to record engine combustion parameters. During the analysis, a specialized software that was based on LAB view was utilized. This program was responsible for monitoring important metrics such as the flow rate of the engine coolant, the flow rate of the air, the temperature within the cylinder, the revolutions per minute, and the temperature readings of the exhaust gas.

Table 3. Engine specification for stationary and modified CRDI mode

| Engine type; 1cylinder, four-stroke compression ignition, @1500, Water cooled | | |
|---|-------------------|----------------------|
| Operating mode | Stationary engine | Modified CRDI engine |
| Bore | 80 mm | 80 mm |
| Stroke | 110 mm | 110 mm |
| Maximum power | 3.7 Kw | 3.7 kW |
| Compression ratio | 18:1 | 19:1, 20:1 and 21:1 |
| Injection pressure (bar) | 200 | 400 |
| Injection timing | 23°bTDC | 23°bTDC |
| Speed | 1500 rpm | 1500 rpm |

After making the necessary adjustments, a Delphi 6-hole nozzle high-pressure solenoid injector was installed in a vertical position on the cylinder head. This was done to prevent fuel spray from striking the cylinder wall. The start of fuel injection timing was kept constant (23° bTDC) for both tests, whereas fuel injection pressure (IP) for the stationary diesel engine was kept constant at 200 bar and for the CRDI it was kept constant at 400 bar with the same engine speed at 1500 rpm. Engine load for the stationary diesel engine test varied from 0 to 25 Nm (with a 5 Nm interval), whereas engine load (50%) was kept constant for the CRDI test. The compression ratio for the stationary engine was fixed at 18:1, while it varied for CRDI mode (19:1, 20:1, and 21:1). To measure engine emissions from the MN-05 model, a MARS portable five-gas emission analyzer was used, whereas smoke opacity was recored with an AVL 437c smoke metre. The initial tests were performed with diesel fuel for the base test reading, followed by KOMÉ fuel with an unmodified and modified engine (Table 3).

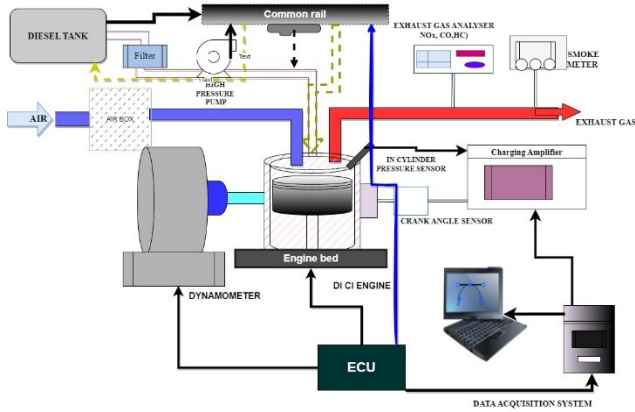


Figure 3. Layout of modified single-cylinder CRDI-Diesel engine

3. Results and discussion

As discussed earlier, the KOME samples were blended and investigated in a stationary and a CRDI-coupled engines. Data obtained from both were compared and the results are discussed in this section. These include engine combustion and emissions characteristics.

3.1. Combustion characteristics

The combustion properties of the KOME blend samples were investigated using the cylinder pressure and heat release curves. As discussed earlier, the engine test setup was attached to a CRDI system capable of injecting high-viscosity fuel at higher IP; hence, the viscosity of biodiesel is no longer a concern for the difference in static and dynamic IP (Winangun *et al.* 2023; Ali and Maki 2023; Kumar and Paul 2023). Therefore, injection angle 23° bTDC was kept constant (as given by the manufacturer) for all the blends and test methods. The start of combustion (SoC) was calculated from the mass fraction burned when 10% of the total fuel mass was burned, and 90% fuel combustion was considered to have occurred at the end of combustion (EoC). (Tutak *et al.* 2023). The SoC for KOME blends (10%, 20%, and 30%) was observed to be earlier than diesel fuel in both stationary and CRDI modes (Figure 4). Even for higher CR 19:1, 20:1, and 21:1 (Figure 4(b)), the SoC for KOME blend samples was advanced due to higher in-cylinder temperature (T_{cyl}) and cetane number (Sharma *et al.* 2021). In CRDI mode at CR20;1, the SoC for KOME 20 was observed to be 1-1.5°CA more advanced than KOME 10 and KOME 30, and 2°CA more advanced than diesel.

In the case of stationary diesel engines, EoC increased with increased fuel blends due to increased fuel viscosity. Higher viscosity decreased combustion efficiency by affecting fuel spray atomization, vaporisation, and the air/fuel mixing ratio (Jindal *et al.* 2010). Sample KOME 30 (30% KOME + 70% diesel) shows the longest combustion duration (CD) (Figure 4(a)) due to higher viscosity. Whereas, in the case of the CRDI mode, EoC was observed to be nearly the same for all the tested fuels at the higher CR, as shown in Figure 4(b). It is because of the higher IP (400 bar) in CRDI mode, which reduces the effect of higher viscosity by producing fine fuel droplets that take less time to vaporise, mix with air, and ignite (Kumar *et al.* 2022).

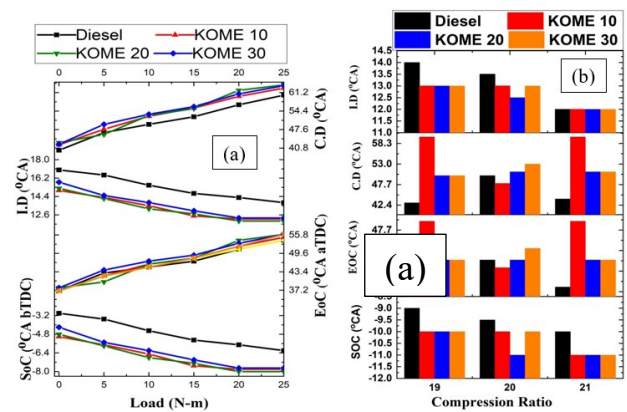


Figure 4. a) Combustion analysis of stationary diesel engine b) CRDI diesel engine

Total combustion initiation time is ignition delay (ID) (Ali and Maki 2023; Kumar and Paul 2023). It is calculated from the difference between the start of injection (SoI) and SoC (Ali and Maki 2023; Kumar and Paul 2023). All the KOME blends show a shorter ID than diesel fuel because of the higher cetane number (Hoang *et al.* 2023) in both the stationary and CRDI modes (Figure 4). The higher IP (400 bar) improved the fuel spray characteristics like spray penetration and fine fuel droplet size (Wai *et al.* 2022). Further, higher CR increases the inlet compressed air temperature, which reduces fuel droplet vaporisation and the air-fuel (A/F) mixing process (Ali and Maki 2023; Jindal *et al.* 2010). The total combustion duration (CD) was perceived to be longer for KOME blends in contrast to diesel fuel in both cases (stationary and CRDI diesel engines), and it increased with an increased blend ratio, as shown in Figure 4 (a) and (b). It is because of the shorter ID, which reduced the duration of the premixed combustion phase (PCP) and extended the diffusion combustion phase (DCP) (Nagaraja *et al.* 2015). The T_{cyl} was dropped in DCP, which reduced the air-fuel mixing rate and resulted in a longer CD (Wai *et al.* 2022). Another reason for the longer CD is the long hydrocarbon chain of fatty acids and double C=C bonds present in the biodiesel (Sharma *et al.* 2019). The dissociation of these carbon chains required higher energy to decompose (Sharma *et al.* 2019). Sharma *et al.* (2019), investigated the effect of shorter and longer carbon chains on engine combustion and emissions characteristics. They reported that biodiesel contains a higher percentage of long carbon chain (C14–C22) fatty acids with double bonds and requires higher energy for complete combustion. Therefore, they produced a longer combustion duration (Sharma *et al.* 2019).

3.2. Cylinder pressure and heat release analysis

The maximum cylinder pressure (P_{max}) and rate of heat release (HRR $_{max}$) at stationary diesel engines are presented in Figure 5(a). Figure 6 shows the deviation of in-cylinder pressure (P_{cyl}) concerning crank angle in the stationary diesel engine. It was detected that P_{cyl} increased with increased engine load (Sriram *et al.* 2023). It was also observed that all the KOME blends show a higher P_{cyl} than diesel at no load and medium load conditions, but it is closer to diesel at full load (Figure 6a–d). The longer ID period of diesel fuel (Figure 4a), which permits more fuel to

burn in PCP, increases the P_{cyl} of diesel fuel closer to KOME blends at full load (Figure 6e–f). It is due to the higher T_{cyl} at full load (25 Nm), which improved the air/fuel mixing rate and made more fuel get burned in the PCP (Tutak *et al.* 2023). The heat release rate (HRR) is used to measure the combustion efficiency by the rate of fuel burn in the PCP (Al-Ansari *et al.* 2023). The PCP can be observed from the HRR curve, as shown in Figure 7(a–f). It was observed that KOME blends showed a lower rate of heat release (HRR) than lower in calorific value than diesel fuel. Furthermore, the higher viscosity of KOME affects the fuel spray characterization and air-fuel mixing rate, which reduces the overall combustion efficiency of KOME blends as compared to diesel fuel in stationary engine mode. Therefore, diesel fuel shows a higher HRRmax than KOME blend, as shown in Figure 6(a). Amongst KOME blends, KOME30 shows a higher HRR of about 5–11% than KOME10 and 20 at medium (10 and 15 Nm) and full load (20 and 25 Nm) due to a higher CV and lower viscosity.

In the case of CRDI engine mode, a higher CR developed a higher P_{cyl} , as shown in Figure 5(b). It found that KOME blends revealed higher P_{cyl} at CR 19:1, 20:1, and 21:1 than diesel, as shown in Figure 8. The reason for the higher P_{cyl} of blended samples is because of a higher cetane number, fuel-bound oxygen %, and higher compressed air temperature, which may reduce the SoC and ID while improving the combustion efficiency (Sharma *et al.* 2021). From Figure 8a, 8b, and 8c, it was observed that P_{cyl} rose with increasing the KOME blend ratios. For example, P_{max} for KOME blends was observed in the sequence KOME 30 > KOME 20 > KOME 10 > Diesel at CR 19:1 and 21:1; whereas KOME 20 shows a lower P_{max} than KOME 10 and KOME 30

but a higher P_{max} in comparison to diesel, as shown in Figure 5(b), respectively.

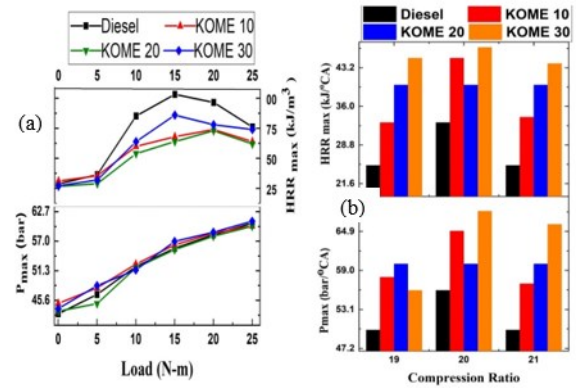


Figure 5. Maximum pressure and heat released rate of stationary diesel engine (a) and CRDI diesel engine (b)

From Figure 8, it is observed that all the KOME blends show higher HRR as compared to diesel fuel. The HRR increased by increasing the diesel ratio (10–30%); it can be seen that the HRR for KOME 30 > KOME 20 > KOME 10 > Diesel (Figure 8). This phenomenon can be characterised by fuel-bound oxygen (Jin and Wei 2023), higher CV, IP, and CR. Higher IP (400 bar) at higher CRs in CRDI mode improved KOME fuel spray penetration and reduced fuel droplet size (Kumar *et al.* 2019). Hence, improved air/fuel mixing rates increased combustion efficacy (Kumar *et al.* 2019). The HRRmax for all the blends was observed to be almost the same at CR 19:1, 20:1, and 21:1, as shown in Figure 5(b). No significant difference was observed in HRRmax with increased CRs of the engine being operated.

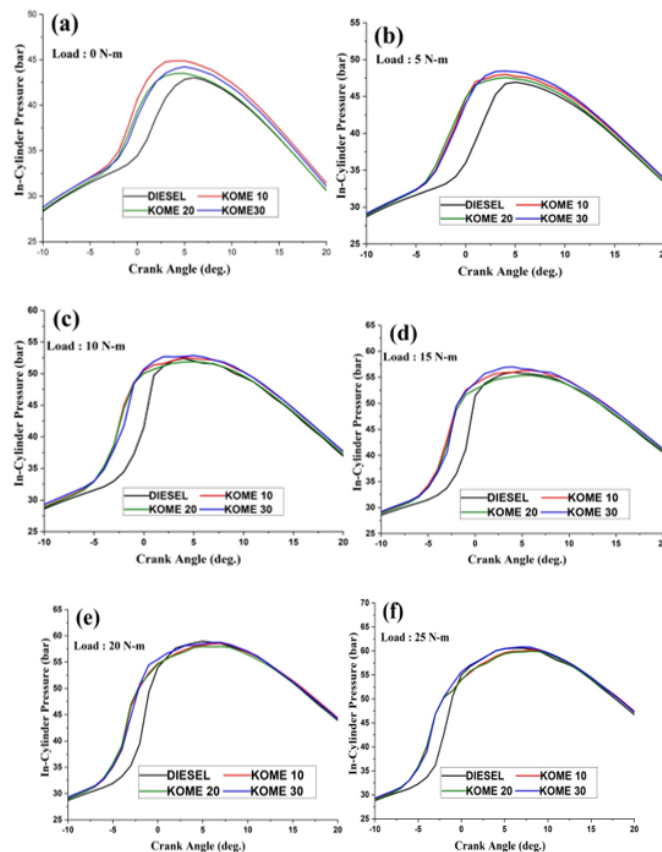


Figure 6. Stationary engine; in-cylinder pressure analysis with crank angle

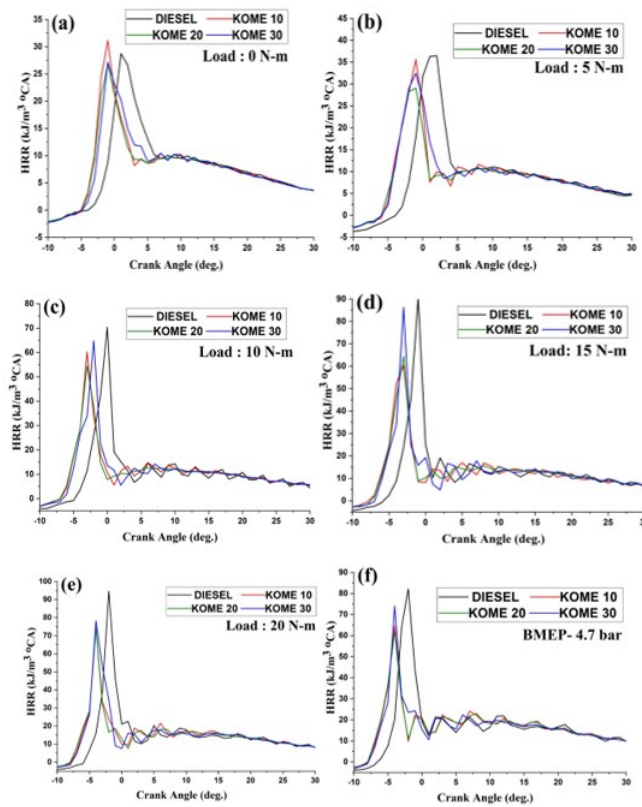


Figure 7. stationary engine; cylinder pressure analysis with crank angle

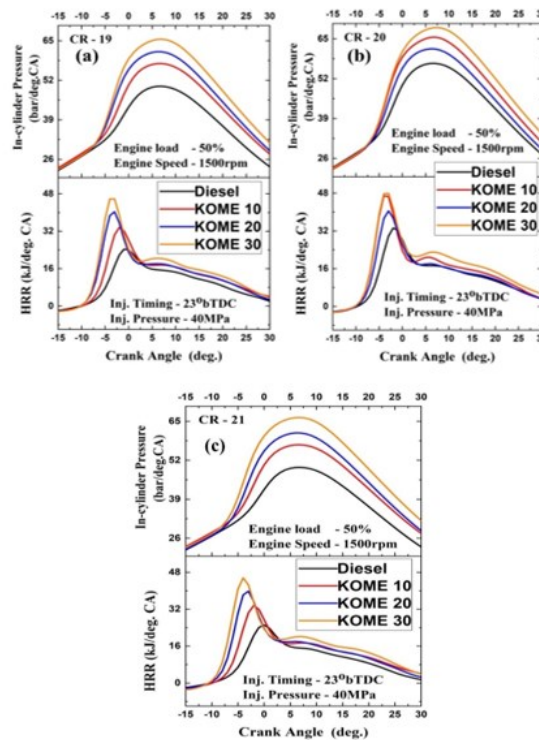


Figure 8. shows the in-cylinder pressure and heat release rate analysis for modified CRDI system

4. Emission characteristics

4.1. Nitric Oxide emission

NOx emissions in biodiesel are the product of the in-cylinder temperature of combustion and fuel-bound radicals (Tutak *et al.* 2023). At higher temperatures, N₂ reacts with O₂ and gives 2NO (Tutak *et al.* 2023). In diesel engines, T_{cyl} increased with increased engine load (Kumar *et al.* 2019), and NOx formed in PCP. In the case of

stationary diesel engine mode, Figure 9(a) shows that KOME blends show higher NOx emissions at no load and medium load conditions, but they decrease at full load (25 Nm). Due to rich F/A ratio at full load propomote incomplete combustion and reduced the T_{cyl} (Sharma *et al.* 2021; Jindal *et al.* 2010). This fall in T_{cyl} reduced the oxidation rate of fuel radicals and slowed the formation of thermal NOx (Channappagoudra and Ramesh 2018; Nagaraja *et al.* 2015). It is clearly seen from Figure 9(a) that

the formation of NO_x is following the same pattern as HRR: KOME 30 > KOME 20 > KOME 10 > Diesel, as discussed in the above section. NO_x emissions were also observed to be higher in CRDI mode at CR 19:1, 20:1, and 21:1, as shown in Figure 9(b). The reason for higher NO_x formation in CRDI mode is due to improved combustion efficiency (Jindal *et al.* 2010). At CR 19:1, NO_x emissions of blends (KOME10, KOME20, and KOME30) were observed to be 2.5%, 1.3%, and 2.7% higher than diesel at CR 19:1, 3.5%, 4.8%, and 3.7% higher than diesel at CR 20:1, and 6.5%, 8.2%, and 6.4% greater than diesel fuel at CR 21:1, as shown in Figure 9(b).

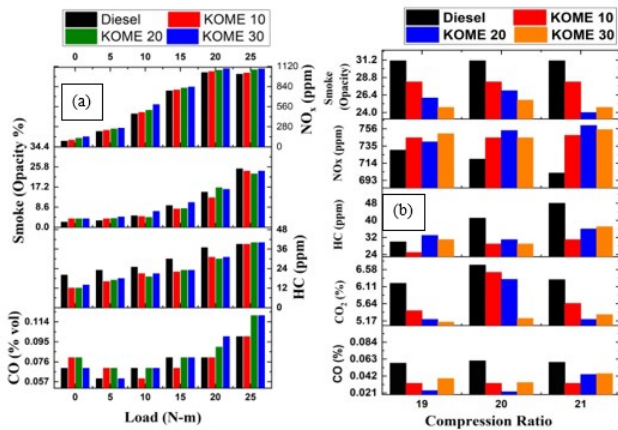


Figure 9. NO_x Comparison of stationary diesel engine (a) and CRDI diesel engine (b)

4.2. Smoke opacity

The smoke opacity percentage for stationary and CRDI diesel engines was observed to be lower, as shown in Figure 9. For stationary engine mode (Figure 9a), it was observed that smoke emission increased with increased engine load due to augmented fuel quantity per stroke (Sharma *et al.* 2022a) but decreased at higher loads due to better combustion efficiency. Smoke emissions for KOME blends were found to be 2–5% higher than diesel fuel at low engine loads (0–5 Nm) due to low T_{cyl} and then decreased about 3–7% at higher loads (10–25 Nm) as compared to diesel fuel due to increased T_{cyl} , which improved fuel combustion. In CRDI mode (Figure 9b), KOME blends show lower smoke emissions than diesel fuel at all CRs, and they are reduced with a rise in the diesel blend ratio (10–30%). Higher IP at higher CRs increases the combustion efficiency of KOME blends due to improved fuel spray characteristics (Nagaraja *et al.* 2015). Sample KOME30 shows 60% lower smoke as compared to KOME10 and KOME20 at all CRs, as shown in Figure 9(b). Smoke emissions of KOME10, KOME20, and KOME30 were observed to be lower by 9%, 16%, and 20% at CR 19:1, 9%, 13%, and 17% at CR 20:1, and 9%, 22%, and 20% at CR 21:1 than diesel, as exposed in Figure 9(b).

4.3. CO and CO₂ Emission

The formation of CO refers to incomplete combustion and a lower rate of oxidation to CO₂ (Vallinayagam *et al.* 2014; Sharma *et al.* 2021). In stationary diesel engine mode (Figure 9a), the formation of CO emissions increased at low load (0–5 Nm) and decreased at medium load (10–15 Nm),

then increased at higher load (20–25 Nm), as shown in Figure 9a. Higher CO at low and higher loads is due to incomplete combustion (Sharma *et al.* 2022a; Nagaraja *et al.* 2015). CO is higher at low loads due to insufficient temperature for CO oxidation to CO₂, whereas CO increases at high loads due to the difficulty of oxygen (rich fuel mixture) for CO oxidation to CO₂. Overall, KOME10 shows a lower CO of about 2–6% than KOME20 and KOME30. In CRDI mode (Figure 9b), all the blends show lower CO and CO₂ than diesel at all higher CRs. In CRDI mode, fuel combustion efficiency increased due to higher IP, whereas higher CRs increased T_{cyl} , resulting in a decrease in the formation of CO emissions (Jindal *et al.* 2010). The CO emissions for KOME10, KOME20, and KOME30 were observed to be lower by 66%, 75%, and 60% at CR 19:1, 59%, 78%, and 58% at CR 20:1, and 66%, 55%, and 54% at CR 21:1 in contrasted to diesel (Figure 9b). Whereas CO₂ emissions for KOME10, KOME20, and KOME30 were reduced by 12%, 15%, and 17% at CR 19:1, 3%, 6%, and 22% at CR 20:1, and 10%, 17%, and 15% at CR 21:1, compared to diesel fuel.

4.4. Un-burnt hydrocarbon emission

Biodiesel exhibited lower hydrocarbon (HC) emissions than diesel due to higher oxygen molecules and cetane numbers, which complete the combustion process and reduce HC emissions (Sharma *et al.* 2022a; Jindal *et al.* 2010). Figure 9(a) shows the formation of HC emissions produced by stationary diesel engines. The formation of HC emissions increased with increased engine load due to incomplete combustion (Sharma *et al.* 2022a; Jindal *et al.* 2010). HC emissions for KOME blends were observed to be lower by 5–15% than diesel at low and medium engine loads. But it increased at full load by about 1.2–1.4% due to the rich fuel/air mixture, which results in incomplete combustion. In CRDI mode (Figure 9b), HC emission of blends KOME10, KOME20, and KOME30 was observed to be lower by 29%, 24%, and 29% at CR20:1 and 35%, 25%, and 35% at CR 21:1 than diesel, as shown in Figure 9(b). Overall, KOME10 shows a lower HC emission of about 20–35% at all CRs.

5. Conclusions

The following conclusions were observed: All the measured and calculated fuel properties of KOME blends were found within the ASTM biodiesel standard limits. In stationary mode, KOME10 and KOME20 show better combustion characteristics, such as shorter SoC and ID and lower P_{max} and HRR, than diesel fuel. Whereas in CRDI mode, all the blends show shorter SoC and ID, but P_{max} and HRR_{max} increase due to higher CR and IP. High CR and IP improved the fuel penetration and spray formation characteristics, resulting in better combustion. As compared to stationary diesel engines, KOME blends had better emissions characteristics. HC, smoke, CO, and CO₂ were found to be lower than diesel fuel, but NO_x was higher due to higher premixed combustion. Overall, KOME20 blend shows a better performance interms of combustion and emissions. Hence, based on the experimental study, KOME20 blend was detected to be a suitable replacement for fossil diesel

fuel in a non-road diesel engine to produce sustainable energy for agriculture and construction applications. Conducting the same test on an on-road automotive engine could be the future scope of the research work.

Declaration of Competing Interest

The authors declare that they have no known competing financial interests or personal relationships that could have appeared to influence the work reported in this paper.

References

- Al-Ansari M.M, Al-Humaid L, Al-Dahmash N.D, Aldawsari M. (2023) Assessing the benefits of *Chlorella vulgaris* microalgal biodiesel for internal combustion engines: Energy and exergy analyses. *Fuel*, 344.
- Ali N, Maki D.F. (2023) Combustion characteristics of CI engine fueled with WCO biodiesel/diesel blends at different compression ratios and EGR. *Heat Transf.*
- Azad A.K, Doppalapudi A.T, Khan M.M.K, Hassan N.M.S, Gudimetla P. A (2023) Landscape review on biodiesel combustion strategies to reduce emission. *Energy Reports*, **9**, 4413–4436.
- Channappagoudra M.N, Ramesh K, G.M. (2018) Influence of compression ratio on diesel engine fueled with dairy scum oil methyl ester. *AIP Conference Proceedings*, 2039(1).
- Chauhan B.S, Kumar N, Cho H.M. (2012) A study on the performance and emission of a diesel engine fueled with *Jatropha* biodiesel oil and its blends. *Energy*, **37(1)**, 616–622.
- El_Kassaby M, Nemit_allah M.A. (2013) Studying the effect of compression ratio on an engine fueled with waste oil produced biodiesel/diesel fuel. *Alexandria Engineering Journal*, **52(1)**, 1–11.
- El-Adawy M, El-kasaby M, Eldrainy Y.A. (2018) Performance characteristics of a supercharged variable compression ratio diesel engine fueled by biodiesel blends. *Alexandria Engineering Journal*, **57(4)**, 3473–3482.
- Hazar H. (2010) Cotton methyl ester usage in a diesel engine equipped with insulated combustion chamber. *Applied Energy*, **87(1)**, 134–140.
- Hoang A.T, Balasubramanian D, Venugopal I.P, Rajendran V, Nguyen D.T, Lawrence K.R, (2023) A feasible and promising approach for diesel engine fuelled with a blend of biodiesel and low-viscosity Cinnamon oil: A comprehensive analysis of performance, combustion, and exergy. *Journal of Cleaner Production*, 401.
- Jin C, Wei J. (2023) The combined effect of water and nanoparticles on diesel engine powered by biodiesel and its blends with diesel: A review. *Fuel*, 343:127940.
- Jindal S, Nandwana B.P, Rathore N.S, Vashistha V. (2010) Experimental investigation of the effect of compression ratio and injection pressure in a direct injection diesel engine running on *Jatropha* methyl ester. *Applied Thermal Engineering*, 30(5):442-8.
- Jindal S, Salvi B.L. (2012) Sustainability aspects and optimization of linseed biodiesel blends for compression ignition engine. *Journal of Renewable and Sustainable Energy*, 4(4).
- Kumar M, Bhowmik S, Paul A. (2022) Effect of pilot fuel injection pressure and injection timing on combustion, performance and emission of hydrogen-biodiesel dual fuel engine. *International Journal of Hydrogen Energy*, 47(68):29554-67.
- Kumar M, Paul A. (2023) Comparative evaluation of combustion, performance, exergy and emission characteristics in hydrogen-biodiesel dual fuel engine under RCCI mode. *Energy & Environment-Uk*.
- Kumar S, Dinesha P, Rosen M.A. (2019) Effect of injection pressure on the combustion, performance and emission characteristics of a biodiesel engine with cerium oxide nanoparticle additive. *Energy*, 185, 1163–1173.
- Luo Y, He Y.T, Liu C.Z, Liao S.Y. (2023) Combustion characteristics of biodiesel with different dimethyl ether blending strategies. *Fuel*, 332.
- Nagaraja S, Sooryaprakash K, Sudhakaran R. (2015) Investigate the Effect of Compression Ratio Over the Performance and Emission Characteristics of Variable Compression Ratio Engine Fueled with Preheated Palm Oil - Diesel Blends. *Procedia Earth and Planetary Science*, **11**, 393–401.
- Raheman H, Ghadge S.V. (2007) Performance of compression ignition engine with mahua (*Madhuca indica*) biodiesel. *Fuel*, **86(16)**, 2568–2573.
- Saleh H.E. (2009) Effect of exhaust gas recirculation on diesel engine nitrogen oxide reduction operating with jojoba methyl ester. *Renewable Energy*, **34(10)**, 2178–2186.
- Sharma V, Duraisamy G, Cho H.M, Arumugam K, Alosius M.A. (2019) Production, combustion and emission impact of bio-mix methyl ester fuel on a stationary light duty diesel engine. *Journal of cleaner production*, 233:147-59.
- Sharma V, Duraisamy G. (2019) Production and characterization of bio-mix fuel produced from a ternary and quaternary mixture of raw oil feedstock, *Journal of cleaner production*, 221, 271–285.
- Sharma V, Hossain A, Duraisamy G. (2021) Experimental Investigation of Neat Biodiesels' Saturation Level on Combustion and Emission Characteristics in a CI Engine. *Energies*, 14(16).
- Sharma V, Hossain A.K, Duraisamy G, Thomas J.J. (2022a) Sustainable biodiesel from flex-mix feedstock and its combustion in a VCR-CRDI engine with variable exhaust gas recirculation and injection pressure. *Journal of Physics: Energy*, 5(1).
- Sharma V, Hossain A.K, Griffiths G, Duraisamy G, Jacob Thomas J. (2022b) Investigation on yield, fuel properties, ageing and low temperature flow of fish oil esters. *Energy Conversion and Management*, 14.
- Sivalakshmi S, Balusamy T. (2012) Influence of Ethanol Addition on a Diesel Engine Fuelled with Neem Oil Methyl Ester. *International Journal of Green Energy*, **9(3)**, 218–228.
- Sriram K, Murugan P.C, Sathiskumar S, Vishnu Ramesh Kumar R, Jayakrishnan S. (2023) Effects of emission and performance characteristics study of rubber seed biodiesel fueled DI diesel engine fumigated with methanol. *Materials Today: Proceedings*.
- Tongroon M, Putrasari Y, Thongchai S. (2023) Influence of engine operating conditions on effect of ethanol combined with biodiesel in ternary blends on combustion behavior in a compression ignition engine. *Journal of Mechanical Science and Technology*, **37(1)**, 395–409.
- Tutak W, Jamrozik A, Grab-Rogalinski K. (2023) Evaluation of Combustion Stability and Exhaust Emissions of a Stationary Compression Ignition Engine Powered by Diesel/n-Butanol and RME Biodiesel/n-Butanol Blends. *Energies*, 16(4).

- Vallinayagam R, Vedharaj S, Yang W.M, Lee P.S, Chua K.J.E, Chou S.K. (2014) Pine oil–biodiesel blends: A double biofuel strategy to completely eliminate the use of diesel in a diesel engine, *Applied Energy*, **130**, 466–473.
- Wai P, Kanokkhanarat P, Oh B-S, Wongpattharaworakul V, Depaiwa N, Po-ngaen W. (2022) Experimental investigation of the influence of ethanol and biodiesel on common rail direct injection diesel Engine's combustion and emission characteristics. *Case Studies in Thermal Engineering*, **39**, 102430.
- Wang M, Nie K, Cao H, Deng L, Wang F, Tan T. (2014) Biodiesel production by combined fatty acids separation and subsequently enzymatic esterification to improve the low temperature properties. *Bioresource Technology*, **174**, 302–305.
- Winangun K, Setiyawan A, Sudarmanta B. (2023) The combustion characteristics and performance of a Diesel Dual-Fuel (DDF) engine fueled by palm oil biodiesel and hydrogen gas. *Case Studies in Thermal Engineering*, 42.
- Yilbasi Z, Yesilyurt M.K, Arslan M, Yaman H. (2023) Understanding the performance, emissions, and combustion behaviors of a DI diesel engine using alcohol/hemp seed oil biodiesel/diesel fuel ternary blends: Influence of long-chain alcohol type and concentration. *Science and Technology for Energy Transition*, 78.